MINERALOGICAL MAGAZINE, SEPTEMBER 1985, VOL. 49, PP. 539-546

Effects of resolution on the measurement of grain 'size'

R. DEARNLEY

British Geological Survey, Murchison House, West Mains Road, Edinburgh EH9 3LA

ABSTRACT. Measurements of fine-grained dolerites by optical automatic image analysis are used to illustrate the effects of magnification and resolution on the values obtained for grain 'size', grain boundary length, surface area per unit volume, and other parameters. Within the measured range of optical magnifications ($\times 26$ to $\times 3571$) and resolutions (1.20×10^{-3} cm to 8.50×10^{-6} cm), it is found that the values of all grain parameters estimated by chord size analysis vary with magnification. These results are interpreted in terms of the concepts of 'fractal dimensions' introduced by Mandelbrot (1967, 1977). For some comparative purposes the fractal relationships may be of little significance as relative changes of size, surface area, and other parameters can be expressed adequately at given magnification(s). But for many studies, for instance in kinetics of grain growth, the actual diameter or surface area per unit volume is an important dimension. The consequences are disconcerting and suggest that it may be difficult in some instances to specify the 'true' measurements of various characteristics of fine-grained aggregates.

KEYWORDS: image analysis, grain size measurement.

THE values obtained from automatic image analysis measurements, such as grain boundary length and mean chord length, depend upon the magnifications employed and therefore also upon the resolution of the image. As magnification increases, grains of progressively smaller size with finer boundary details can be resolved and measurements of grain boundary length per unit area increase correspondingly. True length (of perimeter or chords) appears indeterminate since it depends upon the linear picture element (pixel) scale unit used. As the pixel size decreases the boundary length tends towards infinity.

Although these features are familiar in the measurements of biological images (Paumgartner *et al.*, 1981; Rigaut, 1983) there is little appreciation or discussion of them as they apply to the measurement of grain 'size' in petrology. The aim here is to outline the concept of 'fractal' dimensions (Mandelbrot, 1967, 1977) and to illustrate its application to the measurement of grain 'size' and grain size distributions by automatic image analysis.

Fractal dimensions. The length of a curve or irregular grain perimeter (P) may be measured in terms of a number of steps (n) of length (x), where

$$P = nx. \tag{1}$$

As the step size x decreases, the apparent length of the perimeter increases. Mandelbrot (1967, 1977) has shown that n is not necessarily a linear function of x and that a general expression relating these quantities is given by

$$n = \lambda x^{-D}. \tag{2}$$

Where D is interpreted as a dimension (1, 2, or 3) and λ is a constant representing the measure of the curve in dimension D.

From (2) it is seen that λ represents the length of curve if $D = 1$, area if $D = 2$ or volume if $D = 3$, i.e.

$$\lambda = nx^{D}. \tag{3}$$

Combining (1) and (2) yields

$$P = \lambda x^{-D} x = \lambda x^{1-D}$$

or
$$\log P = (1-D)\log x + \log \lambda. \tag{4}$$

Thus, a plot of $\log P$ against $\log x$ gives a linear trend with a slope $(1-D)$.

The relationship between pixel size (x) and magnification (M) is given by

$$x = \alpha M^{-1} \tag{5}$$

where α is the pixel size at a magnification of $M = 1$, representing the actual pixel size on the monitor screen.

From (4) and (5)

$$P = \lambda \alpha^{1-D} \cdot M^{D-1}$$

or
$$\log P = \log(\lambda \alpha^{1-D}) + (D-1)\log M \tag{6}$$

which is analogous to (4). Comparing (4) and (6) we see that

$$\frac{P_1}{P_2} = \left|\frac{M_1}{M_2}\right|^{D-1} = \left|\frac{x_1}{x_2}\right|^{1-D}. \tag{7}$$

This result is the desired expression which enables the perimeter value (P_1) determined at a

given resolution (x_1) or magnification (M_1) to be transformed to the appropriate perimeter length (P_2) which would be obtained at a different resolution (x_2) or magnification (M_2).

Mandelbrot (1967, 1977) showed that there are lengths of sinuous curves for which ($1 \leqslant D < 2$) and areas where ($2 \leqslant D < 3$). These (non-integer) values of D are termed 'fractals'.

Measurements. To illustrate the relevance of the fractal concept to the relationships of measured grain parameters and the magnifications at which the measurements are made, a series of chord size distributions have been determined on plagioclase feldspars from three texturally homogeneous fine-grained dolerite specimens from near the margins of large sills:

(1) E 59344; 2 cm from the lower contact of an irregular sill about 80 m in thickness at Tal-y-Fan, near Conway, Gwynedd (NGR SH 7295 7270), North Wales.

(2) E 40452; 2 cm from the upper contact of the Whin Sill (67.3 m in thickness) in the Ettersgill (ET-16) borehole (NGR NY 8927 2907), Durham.

(3) E 40382; 61 cm from the lower contact of the Whin Sill (71.0 m in thickness) in the Allanhead no. 1 borehole (NGR NY 8604 4539), Durham.

These speciments have been chosen to represent both similar grain sizes from different intrusions (1 and 2 above) and also different grain sizes from the same intrusion (2 and 3 above); the measurements will be referred to as data sets 1, 2, and 3.

Three main methods have been proposed for the determination of fractal dimensions. (1) A divider stepping method was the first to be used to measure around the length of an outline, either physically (Mandelbrot, 1967, 1977) or by means of a suitable image analysis computer algorithm (Schwartz and Exner, 1980). Alternatively (2) boundary measurements may be made by image analysis using a sized octagonal element to dilate the boundary by known amounts which correspond to different step lengths (Flook, 1978). A different approach (3) is a chord size distribution method using an image analysing computer at various magnifications.

The latter method is employed in the present study, since this allows rapid acquisition of a large number of chord intercepts using a simple sizing algorithm. It is an indirect method since grain perimeter lengths and other parameters are not measured directly by stepping along the features, but are derived from moments of the chord size distribution (see Table I).

Two-dimensional chord size distributions were measured on thin sections of each specimen using a Quantimet 800 Image Analysis System (Cambridge Instruments Ltd.).

Measurements are made in terms of picture elements (pixels) and, as magnification increases, the ratio of the pixel size to grain size decreases. This results in a smaller effective measuring unit for the delineation of grain boundary length or chord length.

Resolution of the image is limited by the finite

Table I. Parameters derived from chord size distribution measurements.

Parameter	Symbol and Units	Derivation *
Number of grains per unit volume of phase	N_v cm^{-3}	$3\bar{c}(\pi\overline{c^2})^{-1}$
Number of grains per unit area of phase	N_A cm^{-2}	$3\bar{c}(\pi\overline{c^3})^{-1}$
Surface area per unit volume of phase	S_v cm^2/cm^3	$4(\bar{c})^{-1}$
Perimeter per unit area of phase	P_A cm/cm^2	$\pi(\bar{c})^{-1}$
Area fraction	f_A	Σc
Mean chord	$\bar{c}$ cm	$\bar{c}$
Standard deviation of mean chord	$\sigma_{\bar{c}}$ cm	$(\overline{c^2}-(\bar{c})^2)^{\frac{1}{2}}$
Diameter of equivalent surface area sphere	D_s cm	$2(\overline{c^2}(3(\bar{c})^2)^{-1})^{\frac{1}{2}}$
Diameter of equivalent volume sphere	D_v cm	$2(\overline{c^3}(4(\bar{c}))^{-1})^{\frac{1}{3}}$
Mean Perimeter per grain	$\bar{P}$ cm	$\pi^2\overline{c^2}(3(\bar{c})^2)^{-1}$
Mean area per grain	$\bar{A}$ cm^2	$\pi\overline{c^2}(3\bar{c})^{-1}$
Mean volume per grain	$\bar{V}$ cm^3	$\pi\overline{c^3}(3\bar{c})^{-1}$

* $\overline{c^m} = (\Sigma c^m)/N$, where N is the number of chords measured and m = 1,2,3,4.

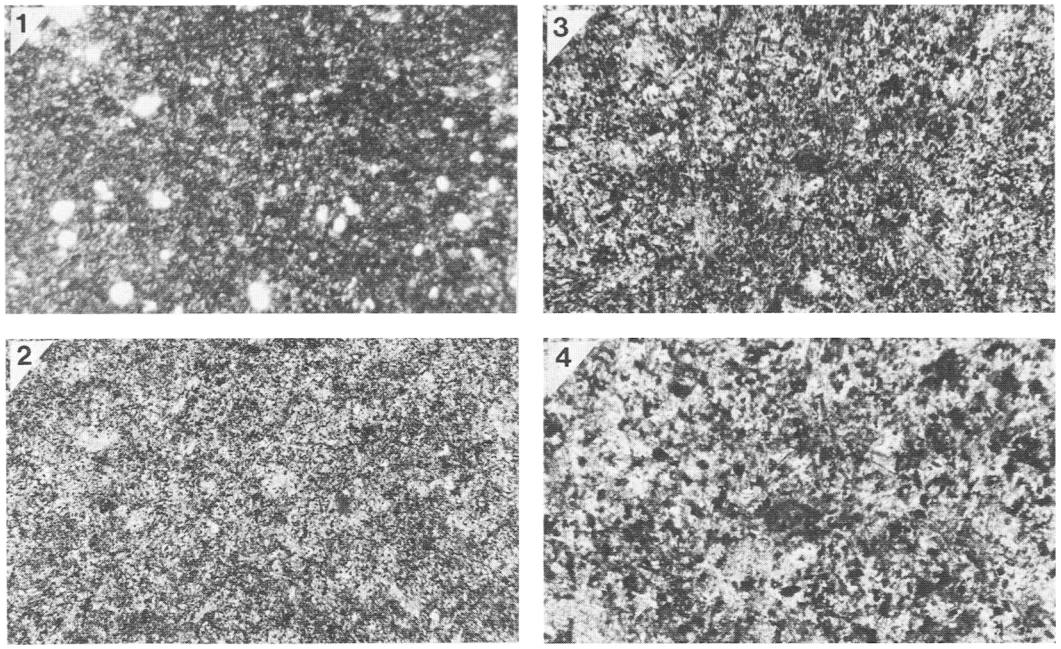

FIG. 1. Plane polarized light photomicrographs of dolerite 61 cm from the lower contact of the Whin Sill (data set 2, see text). The resolutions of these photographs are shown on fig. 4. Magnifications are: 1, ×12; 2, ×30; 3, ×68; 4, ×118.

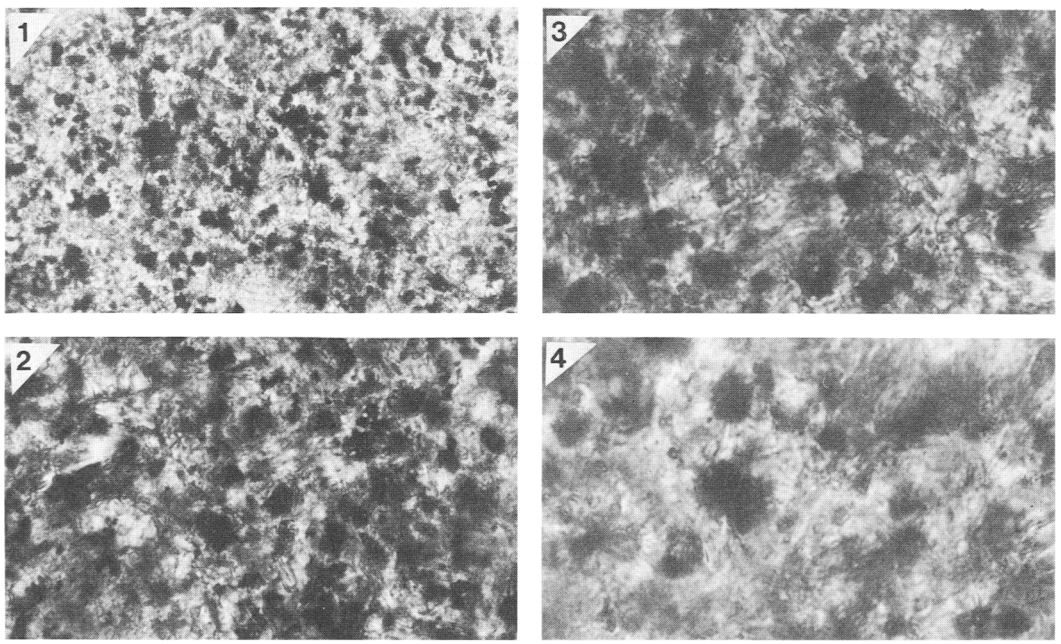

FIG. 2. Plane polarized light photomicrographs of dolerite 61 cm from the lower contact of the Whin Sill (data set 2, see text). The resolution of these photographs are shown on fig. 4. Magnifications are: 1, ×220; 2, ×471; 3, ×706; 4, ×1067.

pixel size on the monitor screen image and by the microscope optics; usually the area of field measured at high magnification is only a sub-area of that for low magnification.

Final magnifications at the monitor screen range from $\times 26$ to $\times 3571$ and as magnification increases the area of thin section covered by a single field of view decreases from 7×10^{-1} cm^2 to 3.6×10^{-5} cm^2. Some examples of the variation of magnification and resolution are shown in figs. 1 and 2.

The detection of any phase, in this instance feldspar, by automatic image analysis is based on a grey-level scale of optical brightness. An automatic setting is used to define the half-contrast grey-level between feldspar and other darker phases, including pyroxenes and opaque oxides. Chord sizing is based upon the measurement of the lengths of horizontal scanning lines (with spacing equal to the resolutions listed in Tables II and III) which intersect the detected areas of feldspar, see fig. 3. A geometric progression of cell sizes for accumulating the chord frequencies between preset (pixel unit) length limits is based on a factor of $(10)^{0.1}$ and this normally results in about 20 or more intervals. All measurements and data collection are under software control.

The first four moments of chord lengths in the two-dimensional image are derived from

$$\overline{c^m} = \Sigma(c^m)/N.$$

Where m is equal to 1,2,3,4; $\Sigma(c^m) = c_1^m + c_2^m + c_3^m \ldots + c_N^m$ and N is the number of chords measured. Tables II and III list these values for the three data sets, each of which consists of measurements taken at a series of different magnifications. A number of different objectives were used ($\times 1$, $\times 2.5$, $\times 5$, $\times 10$, $\times 20$, $\times 40$, $\times 63$, $\times 100$) together with a projector lens assembly which introduced a further magnification factor ($\times 1.000$, $\times 1.195$, $\times 1.532$) to the final monitor screen image; each combination results in a different scanner resolution in cm per pixel (Table II). At all magnifications the optical resolution is superior to that of the scanner and the latter therefore controls the final pixel resolution for the measurements on the monitor screen.

Table II. Magnification, resolution and mean chord measurements, data set 1

Magnification	Resolution cms/pixel	Mean Chords (pixel units) $\overline{c}$	$\overline{c^2}$	$\overline{c^3}$	$\overline{c^4}$
x26	1.20×10^{-3}	9.3	106	1705	42510
x31	1.00×10^{-3}	10.3	127	2112	50954
x38	8.00×10^{-4}	8.7	89	1223	24568
x67	4.55×10^{-4}	10.2	124	2071	51075
x70	4.35×10^{-4}	10.6	135	2340	62043
x81	3.79×10^{-4}	10.5	134	2389	63270
x84	3.66×10^{-4}	11.1	148	2735	35452
x104	2.94×10^{-4}	11.9	177	3875	135123
x110	2.78×10^{-4}	11.2	150	2631	65846
x135	2.27×10^{-4}	11.0	141	2419	61173
x208	1.47×10^{-4}	10.3	126	2071	49959
x253	1.21×10^{-4}	10.8	138	2328	56050
x306	1.00×10^{-4}	10.7	136	2301	53864
x392	7.80×10^{-5}	11.5	163	3158	86853
x478	6.39×10^{-5}	13.3	220	5207	194447
x537	5.70×10^{-5}	13.4	219	4346	121489
x680	4.49×10^{-5}	13.7	223	4721	137018
x927	3.29×10^{-5}	13.8	244	6660	298883
x1133	2.70×10^{-5}	14.6	270	7530	354970
x1165	1.96×10^{-5}	14.5	257	6191	217799
x1392	1.60×10^{-5}	13.6	220	4725	145569
x1457	2.10×10^{-5}	16.1	328	9499	410033
x1785	1.25×10^{-5}	14.8	262	6231	215827
x2318	1.31×10^{-5}	14.5	253	5858	197968
x2807	1.08×10^{-5}	16.8	361	11341	559666
x3571	8.50×10^{-6}	18.7	437	14400	697145

Table III. Magnification, resolution and mean chord measurements, data sets 2 and 3.

Magnification	Resolution cms/pixel	Mean Chords (pixel units) $\overline{c}$	$\overline{c^2}$	$\overline{c^3}$	$\overline{c^4}$
E40452 Data set 2					
x26	1.20×10^{-3}	11.4	148	2383	51582
x70	4.35×10^{-4}	12.0	184	4081	134399
x135	2.27×10^{-4}	11.5	157	2820	71903
x253	1.21×10^{-4}	9.7	110	1597	32141
x478	6.39×10^{-5}	13.7	233	5548	192383
x927	3.29×10^{-5}	12.1	173	3303	90866
x1165	1.96×10^{-5}	10.3	121	1765	35524
E40382 Data set 3					
x26	1.20×10^{-3}	20.6	466	12310	40126
x70	4.35×10^{-4}	18.5	418	12853	57213
x135	2.27×10^{-4}	20.4	550	23201	1621660
x253	1.21×10^{-4}	18.5	462	17906	1085519
x478	6.39×10^{-5}	19.1	494	20359	1329686
x927	3.29×10^{-5}	19.0	478	18229	1083632
x1165	1.96×10^{-5}	21.3	651	34516	3107631

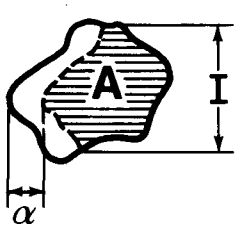

FIG. 3. Chord sizing, showing the effect of measuring all chords $\geqslant \alpha$ pixels across a grain. I = measured intercept, A = measured area. Total length of all chords $\geqslant \alpha = A + I\alpha$.

Since the chord size distribution is based on a two-dimensional scan the logarithmic-cumulative probability plots of the results normally form smooth curves, rather than the straight lines which would be characteristic of a lognormal three-dimensional distribution. Using the method of Cahn and Fullman (1956) the smoothed, two-dimensional frequency distribution may be transformed to the corresponding one in three dimensions; the latter produces a linear trend on a logarithmic cumulative probablity plot indicating the lognormal nature of this chord size distribution.

It becomes increasingly impractical to measure the same area of specimen as magnification increases, but approximately the same number of

chords (about 1.5×10^6) have been measured at each, corresponding to grain boundary lengths per square centimetre ranging from about 2.3 to almost 200 m.

At each magnification the chord length frequency distribution is measured, from which all the other parameters are obtained by the following relationships (Crofton, 1869; Davies, 1962)

$$\bar{c} = \pi \bar{A}/\bar{P} \tag{8}$$

$$\overline{c^3} = 3(\bar{A})^2/\bar{P} \tag{9}$$

where $\bar{c}$ is the mean chord and $\overline{c^3} = (\Sigma c^3)/n$, in which n is the number of chords and $\bar{A}$ and $\bar{P}$ are the mean area and perimeter per grain, expressed as

$$\bar{A} = \pi \overline{c^3}(3\bar{c})^{-1} \tag{10}$$

$$\bar{P} = \pi^2 \overline{c^3}(3(\bar{c})^2)^{-1}. \tag{11}$$

An important additional relationship (Hostinsky, 1925) allows the ratio of mean particle volume ($\bar{V}$) to surface area ($\bar{S}_A$) to be obtained

$$\overline{c^4} = 12\bar{V}^2(\pi S_A)^{-1}. \tag{12}$$

Using this result and that of Cauchy (1850)

$$\bar{c} = 4VS_A^{-1} \tag{13}$$

yields

$$\bar{V} = \pi \overline{c^4}(3c)^{-1} \tag{14}$$

and

$$S_A = 4\pi \overline{c^4}(3(\bar{c})^2)^{-1}. \tag{15}$$

A summary of the derived parameters obtainable from moments of the two-dimensional chord size frequency distribution is given in Table I; although the measured chords are two dimensional (thin section) values the derived estimates of $\bar{V}$, N_v, and S_v are three-dimensional.

Effects of resolution on grain parameter measurements. Previous studies have concentrated mainly on the effects of resolution on measurements of P_A, S_v, and $\bar{P}$ although it is clear that all other grain parameters must also be affected in a corresponding manner.

The principle differences between this study on detected areas of a mineral phase in thin section and others, for instance on biological images, are (i) the extension of the fractal dimensions to other parameters, and (ii) the methods of measurement.

However, if the fractal concept is applied, as outlined above, then values of D may be assigned to the slopes of the log–log plots of various parameters against resolution. On this basis systematic relations between resolution and measurements of various parameters are evident.

Tables II and III list the magnifications and the corresponding resolutions and chord measurements for the three data sets. Least squares regression coefficients (a and b) are given in Table IV for the general form of the relationship $y = ar^b$ where y is the parameter, r is the resolution of the measurement, and b is the slope. Also listed are the values of D derived from $D = (1 \pm b/\delta)$ as shown in Table V, where δ is the appropriate dimension. Log–log plots of the various parameters against resolution for the three data sets are shown in figs. 4–6, and photomicrographs at different resolutions in figs. 1 and 2.

Table IV. Least squares regression coefficients and fractal values for data sets 1–3

Measured Parameter	Least Squares Coefficients		Correlation Coefficient	Fractal Value
	a	b	$\bar{r}$	D_s
Data set 1				
N_v	0.0034	-2.6229	-0.9957	2.87
N_A	0.0320	-1.7490	-0.9969	2.87
S_v	0.9307	-0.8875	-0.9983	2.89
P_A	0.7511	-0.8840	-0.9985	2.88
$\bar{P}$	22.93	0.8628	0.9942	2.86
$\bar{c}$	4.301	0.8875	0.9983	2.89
$\bar{A}$	31.11	1.7490	0.9969	2.87
$\bar{V}$	296.3	2.6229	0.9957	2.87
Data set 2				
N_v	0.0001	-3.0275	-0.9920	3.01
N_A	0.0032	-2.0206	-0.9935	3.01
S_v	0.0121	-1.0173	-0.9877	3.02
P_A	0.2664	-1.0032	-0.9971	3.00
$\bar{P}$	82.54	1.0173	0.9877	3.01
$\bar{c}$	11.79	1.0032	0.9971	3.00
$\bar{A}$	309.9	2.0206	0.9935	3.01
$\bar{V}$	8410	3.0275	0.9920	3.01
Data set 3				
N_v	0.0005	-2.6160	-0.9960	2.87
N_A	0.0054	-1.8100	-0.9979	2.91
S_v	0.2090	-0.9974	-0.9993	3.00
P_A	0.1642	-0.9974	-0.9993	3.00
$\bar{P}$	30.12	0.8125	0.9922	2.81
$\bar{c}$	19.16	0.9975	0.9993	3.00
$\bar{A}$	183.7	1.8100	0.9979	2.91
$\bar{V}$	1881	2.6160	0.9960	2.87

Table V. Mean slopes and fractal values for data sets 1–3

Parameter	Mean Slope (b)	Fractal Values $(1 \pm b/\delta) = D_s$	$D_s = D_T + 1$
N_v	-2.76	1-b/3	1.92	2.92
N_A	-1.86	1-b/2	1.93	2.93
S_v	-0.97	1-b	1.97	2.97
P_A	-0.96	1-b	1.96	2.96
$\bar{P}$	0.90	1+b	1.90	2.90
$\bar{c}$	0.96	1+b	1.96	2.96
$\bar{A}$	1.86	1+b/2	1.93	2.93
$\bar{V}$	2.76	1+b/3	1.92	2.92

Notable features of these plots are the systematic differences in slope and the close approach to linearity, as shown by the correlation coefficients listed in Table IV, although the principal and perhaps most surprising feature is the large range of values for each parameter, depending on the magnifications used in the measurements.

Slopes vary from about 1 for mean grain perimeter ($\bar{P}$) and mean chord ($\bar{c}$) to about 2 for mean grain area ($\bar{A}$) and about 3 for mean grain volume ($\bar{V}$). Corresponding negative slopes occur of about -1 for surface area per unit volume (S_v) and for perimeter per unit area $(P_A)_1$ about -2 for number of grains per unit area, (N_A), about -3 for number of grains per unit volume (N_v). Area fraction has a zero slope and is the only constant measurement with change of resolution.

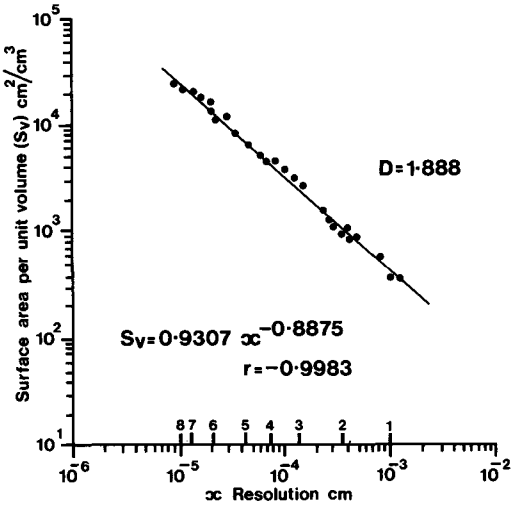

FIG. 4. Variation of surface area per unit volume (S_v) with resolution (x) for data set 1. The fractal value D_2 is equal to 1-slope (see text). Numbers 1-8 refer to resolutions of photographs in figs. 1 and 2.

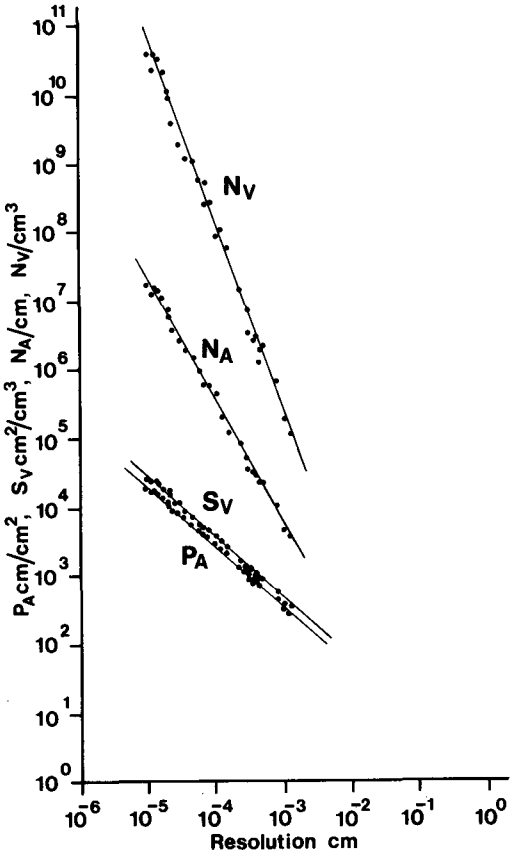

FIG. 5. Mean number of grains/cm^3 (N_v), mean number of grains/cm^2 (N_A), mean surface area per unit volume cm^2/cm^3 (S_v), and mean perimeter per unit area cm/cm^2 (P_A) plotted against the resolution of measurements.

As magnification increases from about $\times 20$ to about $\times 2000$, the apparent mean grain volume $\bar{V}$ and also N_v vary by around six orders of magnitude. $\bar{A}$ and N_A by about three orders of magnitude and S_v, P_A, $\bar{P}$, and $\bar{c}$ by about two orders of magnitude. These extremely large rates of variation with change of magnification are not apparent in reported determinations of grain parameters, since normally only a single magnification is used for the measurements.

The fractal values derived from the relationships given in Table V are listed in Table IV for the three data sets. Fractal dimension obtained from planar measurements (D_2) may be transformed to that (D_3) representing three dimensions by $D_2 + 1 = D_3$ (Paumgartner *et al.*, 1981). On this basis the mean surface area per unit volume (S_v) value of D_3 (Table V) becomes 2.97. The variation in values for D_3 is well illustrated by data from Paumgartner *et al.* (1981) ranging from 2.09, 2.54, 2.72 to the higher values of Table IV of 2.86 to 3.02 (mean 2.97); also by the numerous D_3 values (1.95 to 2.97) listed by Avnir *et al.* (1983).

The results outlined here, as illustrated by the three data sets, are all interrelated by means of the fractal dimension values (Table V) and any parameter (γ) may be transformed from one magnification or resolution to another by means of the relationship

$$\frac{\gamma_1}{\gamma_2} = \left|\frac{M_1}{M_2}\right|^{-b} = \left|\frac{x_1}{x_2}\right|^{b}. \qquad (16)$$

A number of papers refer to fractal dimensions of shapes and surfaces (see Lovejoy, 1982; Avnir *et al.*, 1983) in terms of surface area against diameter or area against perimeter, rather than as relationships of various parameters (Table I) against resolution of the measurements. This study is necessarily confined to the latter presentation, since the

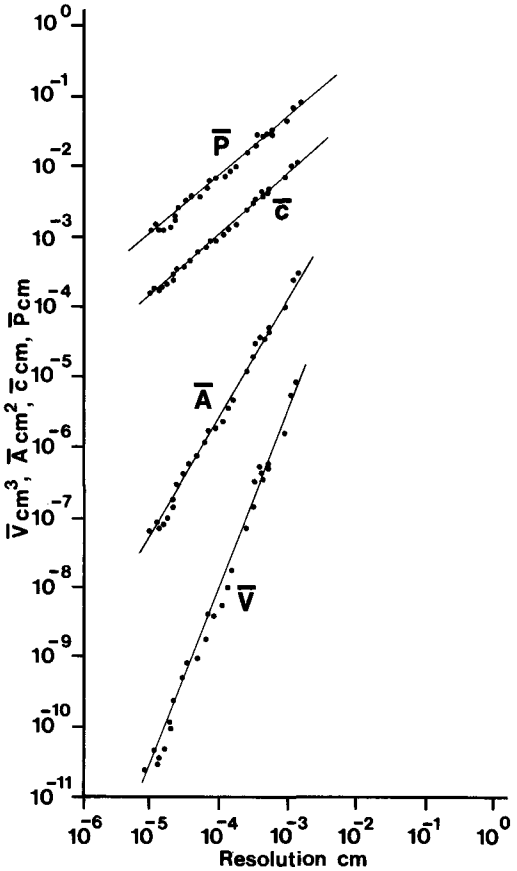

FIG. 6. Mean grain perimeter ($\bar{P}$) cm, mean chord ($\bar{c}$) cm, mean grain area ($\bar{A}$) cm^2, and mean grain volume ($\bar{V}$) cm^3 against resolution of measurements.

measurements are made of chord lengths and all the other parameters are derived from these; hence plotting S_A against D or P against A will yield integer fractals.

The significance of fractal relationships. Discrepancies in S_v and P_A measurements at different magnifications have been noted in various cartographical, biological, and metallurgical systems by Underwood (1961), Richardson (1961), Keller *et al.* (1976), Weibel (1979), Olah (1980), and Paumgartner *et al.* (1981). Weibel (1979) referred to such disturbing findings, commenting that this resolution effect is probably a widespread general phenomenon and that a choice of appropriate resolution was clearly an important consideration in practical stereology.

In some, 'non-ideally fractal', systems (Rigaut, 1983) the log-log relationship of equations (4) and (6) is not followed exactly and at higher magnifications the boundary length asymptotically approaches a maximum value. Increase in length with increasing magnification then ceases to be regular and 'self-similar' and a critical magnification or resolution may be found at which the total complexity of the system is resolved.

Grain parameters recorded here for the three dolerites do not show any departure from a regular (log-log) fractal relationship up to the maximum magnification which can be achieved optically. Theoretically, as magnification increases, the parameters N_v, N_A, S_v, and P_A increase and $\bar{P}$, $\bar{c}$, and $\bar{V}$ decrease without limit.

This paradoxical situation raises a number of problems since, although measurements taken at one magnification can be transformed to those obtainable at another by equation (16), the 'true' dimensions of the structure (to which all measurements should be standardized) remain elusive.

For some comparative purposes the fractal relationships may be of little significance as relative changes of size, surface area, and other parameters can be expressed adequately at given magnification(s). But for many studies, for instance in grain growth kinetics, the actual mean grain diameter or surface area per unit volume is an important dimension in terms of growth and diffusion, since surface free energy and chemical potential gradient are directly related to mean grain curvature and to surface area per unit volume.

Low D_3 values (*c.*2.0) represent relative surface smoothness and high values approaching 3.0 indicate extreme irregularity. The fractal dimension thus becomes a powerful quantitative description of surfaces and also of surface layers, which may vary from a two-dimensional film to an almost three-dimensional bulk as the substrate changes from a near-planar surface to an irregular sponge-like structure in which the adsorbate molecules can penetrate into the solid. These effects are important in surface reactivity and have important applications in surface chemistry (Pfeifer and Avnir, 1983; Avnir *et al.*, 1983, 1984). In a study of fractal surfaces at the molecular level Avnir *et al.* (1984) have collected many examples of high surface area fractal dimensions (2.70–2.97) from a wide range of materials, amongst which are igneous, granitic, and dolomitic rocks.

Application of these concepts to grain growth and to mineral reactions in petrology may yield new and sometimes surprising results as has occurred in other well-established areas of science (Jakeman, 1984). The significance of fractal dimensions is central to the appreciation of all dynamic surface processes dependent on surface irregularities or defects and, as Avnir *et al.* (1984) have pointed out, it is difficult to conceive of any of these processes that are not so dependent.

In a given situation, the thermal history of a rock may result in the attainment of temperatures at which ionic mobility is significant. A reduction of surface area is produced by grain growth, in response to the requirements of minimizing surface energy, in an approach towards equilibrium. In diffusion controlled solid state annealing the mean grain diameter during or after growth (G) is related to the initial diameter (G_0) by the expression

$$G^{1/n} - G_0^{1/n} = kt \qquad (17)$$

where t is time and n is an exponent which may be related to growth mechanisms (Beck, 1948). The temperature dependent growth rate k follows an Arrhenius behaviour

$$k = k_0 \exp(-Q/RT) \qquad (18)$$

where Q is the activation energy for growth, T is temperature, and k_0 is the pre-exponential factor.

In some examples of grain growth the values of n, k, k_0, Q, and T may be derived from the field relationships of grain size to distance (either external or internal) from an igneous contact. The kinetics of grain growth (i) during cooling and annealing growth after crystallization, or (ii) during contact metamorphism, or (iii) during a later phase of regrowth metamorphism may be modelled in this way.

The mean grain diameters used in such relationships (or equivalent sphere diameters, see Table I) determine the estimates of growth rates, activation energy, and temperature under which the reactions occurred. Since the estimated mean grain diameter is dependent upon the magnification and resolution at which measurements are made it is clearly important that the most appropriate or 'relevant' value should be used (Weibel, 1979).

Conclusions. In an ideally fractal relationship the answer to 'what is the appropriate value'? can only be given in terms of the system under consideration. For instance, at one extreme, the mean size of phenocrysts can be adequately defined by including only those larger than a certain size relative to the groundmass; at the other extreme an intrinsic limit to the values of the various parameters is set by the molecular lattice dimensions of the mineral phase (Avnir *et al.*, 1983) at around 10^{-8} cm.

In many instances it does not seem possible to discern a finite limit to the measurements of S_v, P_A, and other parameters at which the structure is completely resolved and it becomes necessary to define a working limit which is appropriate and relevant to the problem in hand. In the study of grain growth reactions the next larger significant scale interval to that of the molecular lattice dimension, relevant to the mechanisms of growth, is given by the mean width of the effective grain boundary regions. Studies of grain boundary width in a variety of materials (see Brady, 1983; Joesten, 1983) yield a range of determined and calculated values, from about 6×10^{-7} cm to about 2×10^{-5} cm, the average of which lies at about 3×10^{-6} cm; for comparison, the highest resolution of the image analysis system (see Table II) is 8.5×10^{-6} cm.

It would seem appropriate to use a resolution near to these values for kinetic studies of the type outlined above, although at present, for ideally fractal relationships, there seems to be no totally satisfactory solution to this perplexing situation. The purpose of this paper is solely to outline the problem and its implications as it applies to granulometric measurements in petrology.

Acknowledgement. This paper is published by permission of the Director, British Geological Survey (NERC).

REFERENCES

Avnir, D., Farin, D., and Pfeifer, P. (1983) *J. Chem. Phys.* **79,** 3566–71.
———————(1984) *Nature*, **308,** 261–3.
Beck, P. A. (1948) *J. Appl. Phys.* **19,** 507–9.
Brady, J. B. (1983) *Am. J. Sci.* **283A,** 181–200.
Cahn, J. W., and Fullman, R. L. (1956) *Trans. AIME*, **206,** 610–12.
Cauchy, A. (1850) *Mem. Acad. Sci. Paris*, **22,** 3.
Crofton, M. W. (1869) *Compt. Rend.* **68,** 1469.
Davies, C. N. (1962) *Nature*, **195,** 768–70.
Flook, A. G. (1978) *Powder Technology*, **21,** 295–8.
Hostinsky, B. (1925) *Publ. Fac. Sci. Univ. Masaryk, Brno*, **50,** 1–26.
Jakeman, E. (1984) *Nature*, **307,** 110.
Joesten, R. (1983) *Am. J. Sci.* **283A,** 233–54.
Keller, H. J. *et al.* (1976) In *Proceedings of the Fourth International Congress on Stereology, Gaithersburg, U.S. Dept of Commerce, National Bureau Standards, Special Publications*, **431,** 409–10.
Lovejoy, S. (1982) *Science*, **216,** 185–7.
Mandelbrot, B. B. (1967) Ibid. **156,** 636–8.
——(1977) *Fractals, Form, Chance, and Dimension.* Freeman, San Francisco.
Olah, A. J. (1980) *Pathol. Res. Pract.* **A166,** 313.
Paumgartner, D., Losa, G., and Weibel, E. R. (1981) *J. Miscroscopy*, **121,** 51–63.
Pfeifer, P., and Avnir, D. (1983) *J. Chem. Phys.* **79,** 3558–65.
Richardson, L. F. (1961) *Gen. Systems Yearbook*, **6,** 139–87.
Rigaut, J. P. (1983) *J. Microscopy*, **133,** 41–54.
Schwartz, H., and Exner, H. E. (1980) *Powder Technology*, **27,** 207–13.
Underwood, E. E. (1961) *Trans. AIME*, **54,** 743.
Weibel, E. R. (1979) *Stereological Methods*, **1,** Academic Press, London.

[*Manuscript received 13 June 1984*]